



www.sciencemag.org/cgi/content/full/335/6072/1058/DC1

Supporting Online Material for

The Geological Record of Ocean Acidification

Bärbel Hönisch,* Andy Ridgwell, Daniela N. Schmidt, Ellen Thomas,
Samantha J. Gibbs, Appy Sluijs, Richard Zeebe, Lee Kump, Rowan C. Martindale,
Sarah E. Greene, Wolfgang Kiessling, Justin Ries, James C. Zachos, Dana L. Royer,
Stephen Barker, Thomas M. Marchitto Jr., Ryan Moyer, Carles Pelejero, Patrizia Ziveri,
Gavin L. Foster, Branwen Williams

*To whom correspondence should be addressed. E-mail: hoenisch@ldeo.columbia.edu

Published 2 March 2012, *Science* **335**, 1058 (2012)
DOI: 10.1126/science.1208277

This PDF file includes:

SOM Text

Figs. S1 to S3

References (74–217)

Other Supporting Online Material for this manuscript includes the following:
(available at www.sciencemag.org/cgi/content/full/335/6072/1058/DC1)

Tables S1 to S3 as an Excel file

Summary of model description (supporting Figure 3)

To illustrate how the different properties of ocean carbonate chemistry vary as the time-scale of atmospheric CO₂ perturbation changes, we use the GENIE Earth system model. GENIE is based on the fast climate model of Edwards and Marsh (79), which features a reduced physics (frictional geostrophic) 3-D ocean circulation model, coupled to a 2-D energy-moisture balance model of the atmosphere and a dynamic-thermodynamic sea-ice model. The ocean model includes a representation of marine carbon cycling, based on a phosphate control of biological productivity, which has been calibrated against observational datasets of ocean geochemistry (80). Of particular relevance to this study is the inclusion of a model of the preservation and burial of biogenic carbonates in deep-sea sediments (81), also calibrated against observations of modern surface sediment composition. Here we additionally include a simple weathering scheme – summarized in Archer et al. (82) but described in full below.

For traceability, the configuration of the model and parameter values employed here are identical to that described in (81). In this: the sediment model is run on the same 36×36 grid as the ocean circulation model, which has 8 levels in the vertical and is forced by annual average wind stress and solar insolation. The carbonate sedimentary preservation model employed follows the ‘look-up table’ approach of (83). The ocean circulation model is run at 100 time-steps per year, with the ocean carbon cycle updated at 25 time-steps per year, and the sediments once per year. The only substantive difference compared to the model described and evaluated in (81) is the use of a more realistic representation of sediment porosity, as described in (84).

As summarized in Archer et al. (82), a simple terrestrial weathering feedback is implemented in GENIE. To configure the weathering scheme, the total pre-industrial weathering flux to the ocean of 11.2 Tmol C yr⁻¹ (diagnosed as that balancing the global burial rate of CaCO₃ in deep-sea sediments – see ‘Summary of model spin-up’, below) is first separated into components related to carbonate and silicate rock weathering. An equal partitioning between alkalinity derived from carbonate and silicate weathering is assumed here, although it should be noted that there is some uncertainty as to what the modern ratio should be with GCM-based geochemical simulations predicting a silicate weathering contribution ranging from 38% to 61% (85).

To balance the removal of carbon from the surficial reservoir via silicate weathering, a constant CO₂ out-gassing flux from volcanic and metamorphic sources ($f_0(\text{CO}_2)$) of 5.6 Tmol C yr⁻¹ is prescribed. The equations describing the net DIC (f_{DIC}) and ALK (f_{ALK}) fluxes to the ocean are:

$$f_{\text{DIC}} = r_{\text{CaCO}_3} \cdot f_0(\text{CaCO}_3) + f_0(\text{CO}_2) \quad (1)$$

$$f_{\text{ALK}} = r_{\text{CaCO}_3} \cdot 2 \cdot f_0(\text{CaCO}_3) + r_{\text{CaSiO}_3} \cdot 2 \cdot f_0(\text{CaSiO}_3) \quad (2)$$

where $f_0(\text{CaCO}_3)$ is the baseline weathering flux from carbonate minerals (mol Ca²⁺ yr⁻¹) and $f_0(\text{CaSiO}_3)$ that from calcium-silicate minerals. The dependence on (seasonal) mean land surface temperature of the scalar modifiers of carbonate and silicate weathering rate, r_{CaCO_3} and r_{CaSiO_3} , respectively, follow Colbourn (86) (in turn based on Berner (87) and Brady (88)):

$$r_{\text{CaSiO}_3} = e^{0.09(T-T_0)} \quad (3)$$

$$r_{\text{CaCO}_3} = 1 + 0.049 \cdot (T - T_0) \quad (4)$$

where T is the mean land surface air temperature (SAT) predicted in GENIE at each time-step, and T_0 the reference mean (annual average) pre-industrial SAT (here: 8.48°C). No plant productivity modifier of weathering is applied, as the particular version of the GENIE model used here does not include a representation of terrestrial vegetation. In addition, no run-off (rainfall) modifiers are applied.

Description of model spin-up

The complete climate+carbon cycle model is initially spun up for 20 ky, with weathering automatically adjusted to match CaCO_3 burial in deep-sea sediments (a ‘closed’ system), no bioturbational mixing specified in the sediments, and atmospheric $p\text{CO}_2$ continually restored to 278 μatm (and $\delta^{13}\text{C}$ to -6.5‰). We do this to accelerate the time to initial steady-state. Following Ridgwell and Hargreaves (81), a 2nd-stage spin-up is then carried out, with the global CaCO_3 burial rate diagnosed from the 1st-stage spin-up used to inform the total weathering rate in the 2nd-stage. This gives a total burial (and hence weathering) rate of 11.2 Tmol Ca^{2+} yr^{-1} . The 2nd-stage spin-up is run for 50 ky with bioturbational mixing in deep-sea sediments now enabled (84). Atmospheric CO_2 and its isotopic composition continue to be restored to pre-industrial values. However, alkalinity (and hence DIC) in the ocean is free to evolve in response to any imbalance between weathering and sedimentation in the deep sea, making this stage of spin-up an ‘open’ system (81).

The result of the 2-stage spin-up is an atmosphere with $p\text{CO}_2 = 278 \mu\text{atm}$ (prescribed) in equilibrium with mean ocean DIC of 2214 $\mu\text{mol kg}^{-1}$, and alkalinity of 2363 $\mu\text{mol kg}^{-1}$, compared to data-based pre-industrial estimates of 2244 and 2363 $\mu\text{mol kg}^{-1}$, respectively (89). Export production is 9.0 PgC yr^{-1} for POC, consistent with much higher resolution 3D ocean biogeochemical models (90), and 1.3 PgC yr^{-1} for CaCO_3 , which is within the 0.8-1.4 PgC yr^{-1} budget range of Feely et al. (91). Mean sediment surface composition is 34.8 wt% CaCO_3 , close to the observationally-based estimate of around 35 wt% (81) with the corresponding burial rate of 0.14 PgC yr^{-1} (1.1 TmolC yr^{-1}) consistent with the CaCO_3 budget of Feely et al. (91).

Description of model experiments

An ensemble of experiments is created, with each experiment forced by a linear atmospheric $p\text{CO}_2$ increase over a specified time interval, with atmospheric CO_2 held constant thereafter. The interval over which atmospheric $p\text{CO}_2$ increases differs in each experiment. Here we test intervals of: 10, 20, 50, 100, 200, 500, 1000, 2000, 5000, 10000, 20000, 50000, and 100000 years. In each of these experiments atmospheric CO_2 changes from $\times 1$ pre-industrial (278 μatm) to $\times 2$ (556 μatm). Hence, each experiment differs only in the rate of increase in atmospheric $p\text{CO}_2$, which itself is related to CO_2 emissions, albeit in a non-linear and time-varying way. The prescribed trajectories of atmospheric $p\text{CO}_2$ are shown in Figure 3A. All experiments are run for a total of 100,000 years and start at the end of the 2nd stage (open system) spin-up.

For each of the time-scales of atmospheric $p\text{CO}_2$ increase, we have also tested the effect of: (i) omitting both the weathering feedback (i.e. fixed weathering fluxes) and climate feedback (i.e. rising $p\text{CO}_2$ does not lead to surface warming) – ensemble ‘S’, (ii) omitting the weathering feedback but including climate feedback (only) – ensemble ‘CS’, and (iii) including a calcification feedback (i.e. pelagic carbonate production responds to rising $p\text{CO}_2$ and ocean acidification) following (92) (but omitting weathering and climate feedbacks) – ensemble ‘Scal’. We find that the response of ocean chemistry is broadly similar across all ensembles as shown in Figure S1. In the main text, we focus on the case with climate and weathering feedbacks. For each ensemble, a control, in which atmospheric $p\text{CO}_2$ is allowed to freely evolve, is also run (also for 100,000 years). Drift is negligible (<<0.1 ppm in atmospheric CO_2) over this interval in these control experiments.

Accessing model source code and experimental results

The model code for the version of the GENIE model used in this paper (technically called: ‘cGENIE’) can be found here:

<https://svn.ggy.bris.ac.uk/subversion/genie/tags/cgenie-0.9.5>

(svn revision 7128) and includes all configuration and boundary condition files needed to carry out the spin-ups, the control experiments, and all four ensembles.

Contact: Andy Ridgwell (andy@seao2) for access to the svn code repository as well as instructions/advice on installing, compiling, and/or running the experiments. Comprehensive documentation on running the cGENIE model can also be found in the genie-docs directory of the code installation.

The results of the spin-ups, control experiments, and model ensembles can be found here:

http://www.seao2.info/cgenie/results/MS.Science2011.SOM/cgenie_output.rar

(See cGENIE documentation for a description of the model output.)

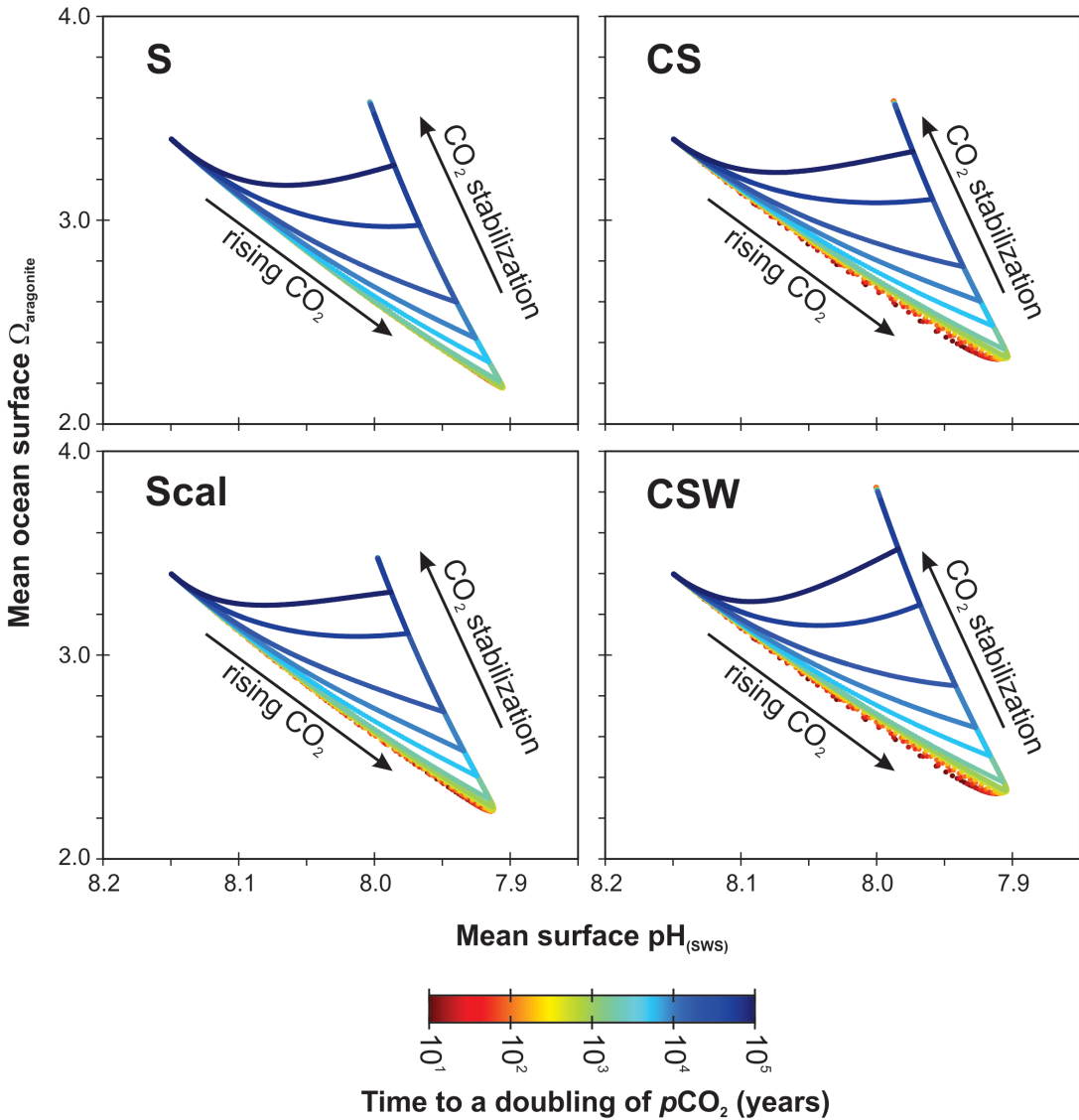


Figure S1. Cross-plots of $\Omega_{\text{aragonite}}$ vs. pH as a function of the rate of $p\text{CO}_2$ increase for the four different Earth system model ensembles. As per Figure 3, the trajectories are color-coded from red (= 'fast') to blue (= 'slow') and represent a range of time-scales for a linear increase in atmospheric $p\text{CO}_2$ from $\times 1$ to $\times 2$ pre-industrial CO_2 . The ensembles are configured as follows: 'S' – sediment only feedback (no climate, calcification, or silicate weathering feedback); 'CS' – sediment and climate feedbacks; 'Scal' – sediment and calcification feedback; and 'CSW' – sediment, climate, and silicate and carbonate weathering feedbacks (as per Figure 3D). See text above for further details.

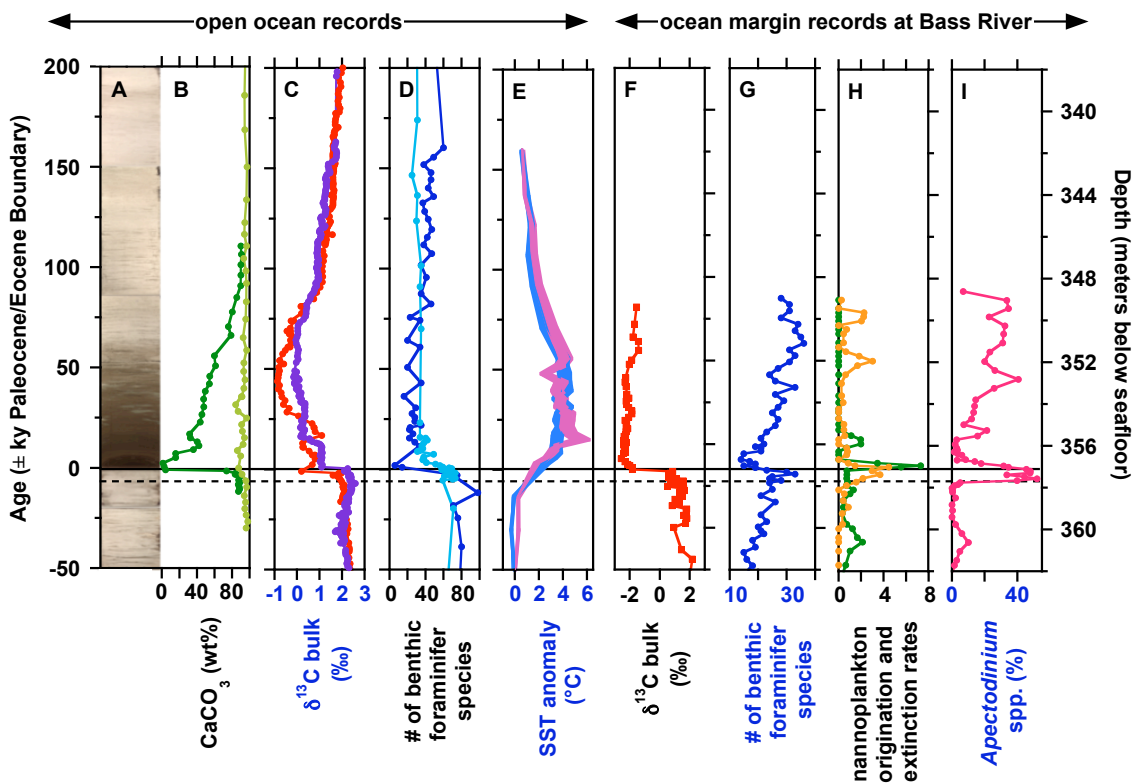


Figure S2. Marine geological and biotic evidence for environmental changes across the PETM in the deep ocean (A-E), and from the ocean margin at Bass River, New Jersey, USA (F-I, ODP Leg 174AX). (A) Sediment core image of ODP 1263 at Walvis Ridge in the South Atlantic (~1500 m paleo-depth), showing typical abrupt replacement of light-colored CaCO_3 by dark clay layer. (B) % CaCO_3 drops to zero at the onset of the event in the South Atlantic [dark green, ODP 1263, (24)] but shows little change on Shatsky Rise in the equatorial Pacific [light green, ODP 1209, (93)], indicating neutralization of acidic seawater along the deep-water flow path (28). (C) Negative carbon isotope excursion (CIE) as recorded in bulk carbonates from ODP 1263 and 1262 [red, (24)] and ODP 690 [purple, (94)]. (D) The number of deep-sea benthic foraminifer species at Walvis Ridge Site 1263 [dark blue, (95)] and Maud Rise Site 690 in the Southern Ocean [light blue, (96)] decreases due to extinction across the PETM. Diversity is particularly low in the Lower CIE assemblage and then gradually recovers over the range of the CIE. (E) Surface ocean warming at ODP Site 1209 from Mg/Ca in two planktic foraminifer species (97). (F) Negative CIE recorded in bulk carbonates from Bass River sediments (98). (G) The number of benthic foraminifers from this outer shelf site is particularly low in the Lower CIE assemblage, reflecting stressed environments, potential seasonal anoxia and high food supply, but extinction is not as severe as in the deep ocean (99). Diversity gradually increases over the range of the CIE. (H) Nannofossil origination (orange) and extinction (green) rates (% per unit depth) at Bass River indicate modest turnover at the onset and peak of the event, consistent with the greatest level of inferred environmental change (37). (I) The quasi-global dominance of the typical low-latitude dinocyst taxon *Apectodinium* during the PETM has been interpreted as the result of global warming and

other factors such as seawater nutrient concentrations, salinity (stratification) and seasonality (34). Note that Bass River data (F-I) are plotted versus core depth (right axis), and correlation to the age scale (in ky relative to the Paleocene/Eocene Boundary, left axis, A-E) is only approximated via carbon isotope records (100). The onset of the *Apectodinium* acme (horizontal dashed line) and warming (based on TEX₈₆, not shown) leads the onset of the CIE (horizontal black line) by ~5,000 years (100), which is consistent with the hypothesis that initial warming caused the injection of ¹³C-depleted carbon by triggering the dissociation of submarine methane hydrates (cf. 101).

Geological or geochemical proxy evidence for	Future & "Anthropocene"	Deglacial Transition	Oligocene – Pliocene	PETM	End Cretaceous	OAEs	Triassic/ Jurassic	Permian/ Triassic
$p\text{CO}_2$ change	↑	↑	↑	↑	↑	↑	↑	↑
pH change	↓	↓	↓	↓	?	?	?	?
Saturation Change	↓	↓	-	↓	↓	?	?	?
Temperature Change	↑	↑	↑	↑	↑	↑	↑	↑
Carbon Release		X	X					
Ocean Acidification Score	/3	2	1	3	1	1.5	2	1.5

Figure S3. The similarity of potential past ocean acidification events to anthropogenic ocean acidification is scored based on geological or geochemical evidence for increased atmospheric $p\text{CO}_2$, decreased pH and carbonate saturation, global warming and massive carbon release from geological reservoirs such as volcanism or fossil carbohydrates. A detailed list of the specific evidence found for each interval is given in Table S1. The extent of change in each parameter is depicted by thick and thin arrows (i.e. strong and weaker evidence, respectively), solid lines indicate geological/geochemical proxy evidence, dashed lines inferred evidence from related parameters, and question marks the lack of independent proxy data. Based on their collective similarity to modern changes, past events are scored, where 3 indicates the greatest alikeness and 1 the lowest.

Additional Data Table S1 (separate EXCEL file)

Climate and/or biotic crises of the past 300 My and inferred ocean acidification. Evidence is cited as supporting the occurrence of ocean acidification across each event: note that biotic responses are often controversial, see text for details. Estimating carbon release rates is hindered by poor age constraints, and only total basalt flows are listed for large igneous provinces after (102). Independent geochemical proxy evidence is rarely available in particular for the ocean but required for unambiguous identification of ocean acidification and reduced carbonate saturation. The similarity of past to modern ocean acidification depends on the magnitude and duration of the CO₂ increase (see Fig. 3), and is scored as in Fig. 4: red = 3 (most similar), orange = 2 (partly similar), yellow = 1 (unlike). Arrows indicate increased ($\uparrow\uparrow$), decreased ($\downarrow\downarrow$) and unchanged/unclear ($\leftrightarrow\leftrightarrow$) conditions associated with each episode. N/A indicates the lack of any published information.

Additional Data Table S2 (separate EXCEL file)

Proxy evidence for varying atmospheric *p*CO₂ throughout the past 300 My (displayed in Fig. 4B). For the Ekart et al. (142) compilation, original sources were used when possible; some data from the Permo-Carboniferous have been supplanted by data from (143) and (144). Most pedogenic carbonate estimates were recalculated using a soil respiration concentration (S[z]) of 2000 ppm (145). Goethite-based CO₂ estimates are excluded due to uncertainties in modeling isotopic fractionation factors (146). Boron isotope-based CO₂ estimates of (147) are excluded due to problems related to diagenesis, vital effects of extinct species, and the evolution of seawater δ¹¹B and alkalinity (63, 148–150). B/Ca CO₂-estimates (151) were excluded due to conflicting apparent controls on the boron partitioning into planktic foraminifer shells (111, 152, 153). Stomatal ratio method calculated as follows: Lower CO₂ bound: 1 SR = 1 RCO₂; upper CO₂ bound: 1 SR = 2RCO₂, where SR = stomatal ratio and RCO₂ is the ratio of CO₂ in the past relative to today [see (154)]; CO₂ baseline = 300 ppm; SI baseline = 12.1%). All liverwort-based estimates are updated using the atmospheric δ¹³C record of (155). Many individual CO₂ estimates are based on multiple measurements of the same material. Consult original literature for details. All dates are calibrated to the timescale of Gradstein et al. (156).

Additional Data Table S3 (separate EXCEL file)

Phanerozoic seawater [Mg²⁺] and [Ca²⁺] from observations (71) and model estimates (72). Data are displayed in Fig. 4D.

References for fossil diversity and geologic distribution shown in Figure 1, including photo credits. Note that Cretaceous dinocyst diversity is studied in greater detail than other periods, possibly biasing evolutionary trends.
Species and credits are listed from left to right for each group of organisms.

Group of organisms and references for fossil diversity	Species	Credit
Organic-walled Dinocysts (213)	<i>Impagidinium aquaductum</i>	Appy Sluijs, Utrecht University
	<i>Apectodinium homomorphum</i>	Appy Sluijs, Utrecht University
Calcareous Nannofossils (22)	<i>Coccolithus pelagicus</i>	Patrizia Ziveri, Universitat Autònoma de Barcelona
	<i>Discoaster</i>	Patrizia Ziveri, Universitat Autònoma de Barcelona
	nannoconid	Paul Bown, University College London
Planktic Foraminifers (214-216)	<i>Globigerinoides sacculifer</i>	Janina Ruprecht, Lamont-Doherty Earth Observatory
	<i>Acarinina</i> sp.	Suzanne Jennions, Bristol University
	<i>Rugoglobigerina rugosa</i>	Brian Huber, Smithsonian Institution
Benthic Foraminifers (215, 217)	<i>Cibicidoides wuellerstorfi</i>	Ellen Thomas, Yale
	<i>Tappanina selmensis</i>	Ellen Thomas, Yale
	<i>Siphonodosaria</i> sp.	Ellen Thomas, Yale
	<i>Triticites secalicus</i>	John Groves, University of Northern Iowa
Shallow Reef Builders (32, 134, 217)	<i>Cladocora caespitosa</i>	Eva Calvo, Institut de Ciències del Mar, CSIC
	<i>Thecosmilia trichotoma</i>	Antje Dittmann, Museum für Naturkunde at Humboldt University

References and Notes

1. A. Ridgwell, D. N. Schmidt, Past constraints on the vulnerability of marine calcifiers to massive carbon dioxide release. *Nat. Geosci.* **3**, 196 (2010). [doi:10.1038/ngeo755](https://doi.org/10.1038/ngeo755)
2. Methods and materials are available as supporting material on *Science* Online.
3. W. H. Berger, *Deep-Sea Res.* **15**, 31 (1968).
4. S. Barker, H. Elderfield, Foraminiferal calcification response to glacial-interglacial changes in atmospheric CO₂. *Science* **297**, 833 (2002). [doi:10.1126/science.1072815](https://doi.org/10.1126/science.1072815) [Medline](#)
5. S. Barker *et al.*, Temporal changes in North Atlantic circulation constrained by planktonic foraminiferal shell weights. *Paleoceanography* **19**, PA3008 (2004). [doi:10.1029/2004PA001004](https://doi.org/10.1029/2004PA001004)
6. S. J. Gibbs, H. M. Stoll, P. R. Bown, T. J. Bralower, Ocean acidification and surface water carbonate production across the Paleocene–Eocene thermal maximum. *Earth Planet. Sci. Lett.* **295**, 583 (2010). [doi:10.1016/j.epsl.2010.04.044](https://doi.org/10.1016/j.epsl.2010.04.044)
7. K. Caldeira, M. E. Wickett, Oceanography: anthropogenic carbon and ocean pH. *Nature* **425**, 365 (2003). [doi:10.1038/425365a](https://doi.org/10.1038/425365a) [Medline](#)
8. An online associated carbonate chemistry tutorial is available as supporting material on *Science* Online.
9. A. Ridgwell, R. E. Zeebe, The role of the global carbonate cycle in the regulation and evolution of the Earth system. *Earth Planet. Sci. Lett.* **234**, 299 (2005). [doi:10.1016/j.epsl.2005.03.006](https://doi.org/10.1016/j.epsl.2005.03.006)
10. D. Archer, H. Kheshgi, E. Maier-Reimer, Multiple timescales for neutralization of fossil fuel CO₂. *Geophys. Res. Lett.* **24**, 405 (1997). [doi:10.1029/97GL00168](https://doi.org/10.1029/97GL00168)
11. E. Monnin *et al.*, Atmospheric CO₂ concentrations over the last glacial termination. *Science* **291**, 112 (2001). [doi:10.1126/science.291.5501.112](https://doi.org/10.1126/science.291.5501.112) [Medline](#)
12. B. Hönisch, N. G. Hemming, Surface ocean pH response to variations in pCO₂ through two full glacial cycles. *Earth Planet. Sci. Lett.* **236**, 305 (2005). [doi:10.1016/j.epsl.2005.04.027](https://doi.org/10.1016/j.epsl.2005.04.027)
13. L. Beaufort *et al.*, Sensitivity of coccolithophores to carbonate chemistry and ocean acidification. *Nature* **476**, 80 (2011). [doi:10.1038/nature10295](https://doi.org/10.1038/nature10295) [Medline](#)
14. J. W. Farrell, W. Prell, Climatic change and CaCO₃ preservation: An 800,000 year bathymetric Reconstruction from the central equatorial Pacific Ocean. *Paleoceanography* **4**, 447 (1989). [doi:10.1029/PA004i004p00447](https://doi.org/10.1029/PA004i004p00447)
15. B. Hönisch, T. Bickert, N. G. Hemming, Modern and Pleistocene boron isotope composition of the benthic foraminifer *Cibicidoides wuellerstorfi*. *Earth Planet. Sci. Lett.* **272**, 309 (2008). [doi:10.1016/j.epsl.2008.04.047](https://doi.org/10.1016/j.epsl.2008.04.047)
16. J. Yu *et al.*, Loss of carbon from the deep sea since the Last Glacial Maximum. *Science* **330**, 1084 (2010). [doi:10.1126/science.1193221](https://doi.org/10.1126/science.1193221) [Medline](#)

17. T. M. Marchitto, J. Lynch-Stieglitz, S. R. Hemming, Deep Pacific CaCO₃ compensation and glacial–interglacial atmospheric CO₂. *Earth Planet. Sci. Lett.* **231**, 317 (2005).
[doi:10.1016/j.epsl.2004.12.024](https://doi.org/10.1016/j.epsl.2004.12.024)
18. O. Seki *et al.*, Alkenone and boron-based Pliocene pCO₂ records. *Earth Planet. Sci. Lett.* **292**, 201 (2010). [doi:10.1016/j.epsl.2010.01.037](https://doi.org/10.1016/j.epsl.2010.01.037)
19. A. M. Haywood *et al.*, Comparison of mid-Pliocene climate predictions produced by the HadAM3 and GCMAM3 General Circulation Models. *Global Planet. Change* **66**, 208 (2009). [doi:10.1016/j.gloplacha.2008.12.014](https://doi.org/10.1016/j.gloplacha.2008.12.014)
20. M. Pagani, Z. Liu, J. LaRiviere, A. C. Ravelo, High Earth-system climate sensitivity determined from Pliocene carbon dioxide concentrations. *Nat. Geosci.* **3**, 27 (2010).
[doi:10.1038/ngeo724](https://doi.org/10.1038/ngeo724)
21. H. J. Dowsett, M. M. Robinson, Mid-Pliocene planktic foraminifer assemblage of the North Atlantic Ocean. *Micropaleontology* **53**, 105 (2007). [doi:10.2113/gsmicropal.53.1-2.105](https://doi.org/10.2113/gsmicropal.53.1-2.105)
22. P. R. Bown *et al.*, in *Coccolithophores – From molecular processes to global impacts*, H. R. Thierstein, J. R. Young, Eds. (Springer, Berlin, 2004), pp. 481-508.
23. J. P. Kennett, L. D. Stott, Abrupt deep-sea warming, palaeoceanographic changes and benthic extinctions at the end of the Palaeocene. *Nature* **353**, 225 (1991).
[doi:10.1038/353225a0](https://doi.org/10.1038/353225a0)
24. J. C. Zachos *et al.*, Rapid acidification of the ocean during the Paleocene-Eocene thermal maximum. *Science* **308**, 1611 (2005). [doi:10.1126/science.1109004](https://doi.org/10.1126/science.1109004) Medline
25. J. C. Zachos, H. McCarren, B. Murphy, U. Röhl, T. Westerhold, Tempo and scale of late Paleocene and early Eocene carbon isotope cycles: Implications for the origin of hyperthermals. *Earth Planet. Sci. Lett.* **299**, 242 (2010). [doi:10.1016/j.epsl.2010.09.004](https://doi.org/10.1016/j.epsl.2010.09.004)
26. R. E. Zeebe, J. C. Zachos, G. R. Dickens, Carbon dioxide forcing alone insufficient to explain Palaeocene–Eocene Thermal Maximum warming. *Nat. Geosci.* **2**, 576 (2009).
[doi:10.1038/ngeo578](https://doi.org/10.1038/ngeo578)
27. K. Panchuk, A. Ridgwell, L. R. Kump, Sedimentary response to Paleocene-Eocene Thermal Maximum carbon release: A model-data comparison. *Geology* **36**, 315 (2008).
[doi:10.1130/G24474A.1](https://doi.org/10.1130/G24474A.1)
28. R. E. Zeebe, J. C. Zachos, Reversed deep-sea carbonate ion basin gradient during Paleocene-Eocene thermal maximum. *Paleoceanography* **22**, PA3201 (2007).
[doi:10.1029/2006PA001395](https://doi.org/10.1029/2006PA001395)
29. E. Thomas, in *Geological Society of America Special Paper*, S. Monechi, R. Coccioni, M. R. Rampino, Eds. (Geological Society of America, 2007), pp. 1-23.
30. F. J. Rodríguez-Tovar, A. Uchman, L. Alegret, E. Molina, Impact of the Paleocene–Eocene Thermal Maximum on the macrobenthic community: Ichnological record from the Zumaia section, northern Spain. *Mar. Geol.* **282**, 178 (2011).
[doi:10.1016/j.margeo.2011.02.009](https://doi.org/10.1016/j.margeo.2011.02.009)

31. C. Scheibner, R. P. Speijer, Late Paleocene–early Eocene Tethyan carbonate platform evolution — A response to long- and short-term paleoclimatic change. *Earth Sci. Rev.* **90**, 71 (2008). [doi:10.1016/j.earscirev.2008.07.002](https://doi.org/10.1016/j.earscirev.2008.07.002)
32. W. Kiessling, C. Simpson, On the potential for ocean acidification to be a general cause of ancient reef crises. *Glob. Change Biol.* **17**, 56 (2011). [doi:10.1111/j.1365-2486.2010.02204.x](https://doi.org/10.1111/j.1365-2486.2010.02204.x)
33. S. J. Gibbs, T. J. Bralower, P. R. Bown, J. C. Zachos, L. M. Bybell, Shelf and open-ocean calcareous phytoplankton assemblages across the Paleocene-Eocene Thermal Maximum: Implications for global productivity gradients. *Geology* **34**, 233 (2006). [doi:10.1130/G22381.1](https://doi.org/10.1130/G22381.1)
34. A. Sluijs, H. Brinkhuis, A dynamic climate and ecosystem state during the Paleocene-Eocene Thermal Maximum: inferences from dinoflagellate cyst assemblages on the New Jersey Shelf. *Biogeosciences* **6**, 1755 (2009). [doi:10.5194/bg-6-1755-2009](https://doi.org/10.5194/bg-6-1755-2009)
35. A. Sluijs *et al.*, Warm and wet conditions in the Arctic region during Eocene Thermal Maximum 2. *Nat. Geosci.* **2**, 777 (2009). [doi:10.1038/ngeo668](https://doi.org/10.1038/ngeo668)
36. I. Raffi, B. De Bernardi, Response of calcareous nannofossils to the Paleocene–Eocene Thermal Maximum: Observations on composition, preservation and calcification in sediments from ODP Site 1263 (Walvis Ridge — SW Atlantic). *Mar. Micropaleontol.* **69**, 119 (2008). [doi:10.1016/j.marmicro.2008.07.002](https://doi.org/10.1016/j.marmicro.2008.07.002)
37. S. J. Gibbs, P. R. Bown, J. A. Sessa, T. J. Bralower, P. A. Wilson, Nannoplankton extinction and origination across the Paleocene-Eocene Thermal Maximum. *Science* **314**, 1770 (2006). [doi:10.1126/science.1133902](https://doi.org/10.1126/science.1133902) Medline
38. P. Schulte *et al.*, The Chicxulub asteroid impact and mass extinction at the Cretaceous-Paleogene boundary. *Science* **327**, 1214 (2010). [doi:10.1126/science.1177265](https://doi.org/10.1126/science.1177265) Medline
39. S. D'Hondt, M. E. Q. Pilson, H. Sigurdsson, A. K. Hanson, Jr., S. Carey, Surface-water acidification and extinction at the Cretaceous-Tertiary boundary. *Geology* **22**, 983 (1994). [doi:10.1130/0091-7613\(1994\)022<0983:SWAAEA>2.3.CO;2](https://doi.org/10.1130/0091-7613(1994)022<0983:SWAAEA>2.3.CO;2)
40. R. E. Zeebe, P. Westbroek, A simple model for the CaCO_3 saturation state of the ocean: The “Strangelove,” the “Neritan,” and the “Cretan” Ocean. *Geochem. Geophys. Geosyst.* **4**, 1104 (2003). [doi:10.1029/2003GC000538](https://doi.org/10.1029/2003GC000538)
41. C. Langdon *et al.*, Effect of calcium carbonate saturation state on the calcification rate of an experimental coral reef. *Global Biogeochem. Cycles* **14**, 639 (2000). [doi:10.1029/1999GB001195](https://doi.org/10.1029/1999GB001195)
42. H. C. Jenkyns, Geochemistry of oceanic anoxic events. *Geochem. Geophys. Geosyst.* **11**, Q03004 (2010). [doi:10.1029/2009GC002788](https://doi.org/10.1029/2009GC002788)
43. R. M. Leckie *et al.*, Oceanic anoxic events and plankton evolution: Biotic response to tectonic forcing during the mid-Cretaceous. *Paleoceanography* **17**, 1041 (2002). [doi:10.1029/2001PA000623](https://doi.org/10.1029/2001PA000623)
44. E. Erba, F. Tremolada, Nannofossil carbonate fluxes during the Early Cretaceous: Phytoplankton response to nutrification episodes, atmospheric CO_2 , and anoxia. *Paleoceanography* **19**, PA1008 (2004). [doi:10.1029/2003PA000884](https://doi.org/10.1029/2003PA000884)

45. E. Erba, C. Bottini, H. J. Weissert, C. E. Keller, Calcareous nannoplankton response to surface-water acidification around Oceanic Anoxic Event 1a. *Science* **329**, 428 (2010). [doi:10.1126/science.1188886](https://doi.org/10.1126/science.1188886) [Medline](#)
46. S. J. Gibbs, S. A. Robinson, P. R. Bown, T. D. Jones, J. Henderiks, Comment on “Calcareous nannoplankton response to surface-water acidification around Oceanic Anoxic Event 1a”. *Science* **332**, 175, author reply 175 (2011). [doi:10.1126/science.1199459](https://doi.org/10.1126/science.1199459) [Medline](#)
47. G. Suan *et al.*, Duration of the Early Toarcian carbon isotope excursion deduced from spectral analysis: Consequence for its possible causes. *Earth Planet. Sci. Lett.* **267**, 666 (2008). [doi:10.1016/j.epsl.2007.12.017](https://doi.org/10.1016/j.epsl.2007.12.017)
48. A. S. Cohen, A. L. Coe, D. B. Kemp, The Late Palaeocene Early Eocene and Toarcian (Early Jurassic) carbon isotope excursions: a comparison of their time scales, associated environmental changes, causes and consequences. *J. Geol. Soc. London* **164**, 1093 (2007). [doi:10.1144/0016-76492006-123](https://doi.org/10.1144/0016-76492006-123)
49. E. Mattioli, B. Pittet, L. Petitpierre, S. Mailliot, Dramatic decrease of pelagic carbonate production by nannoplankton across the Early Toarcian anoxic event (T-OAE). *Global Planet. Change* **65**, 134 (2009). [doi:10.1016/j.gloplacha.2008.10.018](https://doi.org/10.1016/j.gloplacha.2008.10.018)
50. J. H. Whiteside, P. E. Olsen, D. V. Kent, S. J. Fowell, M. Et-Touhami, Synchrony between the Central Atlantic magmatic province and the Triassic–Jurassic mass-extinction event? *Palaeogeogr. Palaeoclimatol. Palaeoecol.* **244**, 345 (2007). [doi:10.1016/j.palaeo.2006.06.035](https://doi.org/10.1016/j.palaeo.2006.06.035)
51. D. B. Kemp, A. L. Coe, A. S. Cohen, L. Schwark, Astronomical pacing of methane release in the Early Jurassic period. *Nature* **437**, 396 (2005). [doi:10.1038/nature04037](https://doi.org/10.1038/nature04037) [Medline](#)
52. M. Ruhl, N. R. Bonis, G. J. Reichart, J. S. Sininghe Damsté, W. M. Kürschner, Atmospheric carbon injection linked to end-Triassic mass extinction. *Science* **333**, 430 (2011). [doi:10.1126/science.1204255](https://doi.org/10.1126/science.1204255) [Medline](#)
53. A. E. Crne, H. Weissert, S. Gorican, S. M. Bernasconi, A biocalcification crisis at the Triassic–Jurassic boundary recorded in the Budva Basin (Dinarides, Montenegro). *Geol. Soc. Am. Bull.* **123**, 40 (2011). [doi:10.1130/B30157.1](https://doi.org/10.1130/B30157.1)
54. J. L. Payne *et al.*, *Proc. Nat. Acad. Sci.* **107**, 8543 (2010).
55. S. V. Sobolev *et al.*, Linking mantle plumes, large igneous provinces and environmental catastrophes. *Nature* **477**, 312 (2011). [doi:10.1038/nature10385](https://doi.org/10.1038/nature10385) [Medline](#)
56. S. Z. Shen *et al.*, Calibrating the end-Permian mass extinction. *Science* **334**, 1367 (2011). [doi:10.1126/science.1213454](https://doi.org/10.1126/science.1213454) [Medline](#)
57. C. Le Quéré *et al.*, Trends in the sources and sinks of carbon dioxide. *Nat. Geosci.* **2**, 831 (2009). [doi:10.1038/ngeo689](https://doi.org/10.1038/ngeo689)
58. P. B. Wignall, S. Kershaw, P.-Y. Collin, S. Crasquin-Soleau, Erosional truncation of uppermost Permian shallow-marine carbonates and implications for Permian-Triassic boundary events: Comment. *Geol. Soc. Am. Bull.* **121**, 954 (2009). [doi:10.1130/B26424.1](https://doi.org/10.1130/B26424.1)

59. A. H. Knoll, R. K. Bambach, J. L. Payne, S. Pruss, W. W. Fischer, Paleophysiology and end-Permian mass extinction. *Earth Planet. Sci. Lett.* **256**, 295 (2007). [doi:10.1016/j.epsl.2007.02.018](https://doi.org/10.1016/j.epsl.2007.02.018)
60. J. Zachos, M. Pagani, L. Sloan, E. Thomas, K. Billups, Trends, rhythms, and aberrations in global climate 65 Ma to present. *Science* **292**, 686 (2001). [doi:10.1126/science.1059412](https://doi.org/10.1126/science.1059412) [Medline](#)
61. Y. Cui *et al.*, Slow release of fossil carbon during the Palaeocene–Eocene Thermal Maximum. *Nat. Geosci.* **4**, 481 (2011). [doi:10.1038/ngeo1179](https://doi.org/10.1038/ngeo1179)
62. M. Ruhl *et al.*, Astronomical constraints on the duration of the early Jurassic Hettangian stage and recovery rates following the end-Triassic mass extinction (St Audrie's Bay/East Quantoxhead, UK). *Earth Planet. Sci. Lett.* **295**, 262 (2010). [doi:10.1016/j.epsl.2010.04.008](https://doi.org/10.1016/j.epsl.2010.04.008)
63. D. Lemarchand, J. Gaillardet, E. Lewin, C. J. Allègre, The influence of rivers on marine boron isotopes and implications for reconstructing past ocean pH. *Nature* **408**, 951 (2000). [doi:10.1038/35050058](https://doi.org/10.1038/35050058) [Medline](#)
64. R. M. Coggon, D. A. Teagle, C. E. Smith-Duque, J. C. Alt, M. J. Cooper, Reconstructing past seawater Mg/Ca and Sr/Ca from mid-ocean ridge flank calcium carbonate veins. *Science* **327**, 1114 (2010). [doi:10.1126/science.1182252](https://doi.org/10.1126/science.1182252) [Medline](#)
65. M. F. Stuecker, R. E. Zeebe, Ocean chemistry and atmospheric CO₂ sensitivity to carbon perturbations throughout the Cenozoic. *Geophys. Res. Lett.* **37**, L03609 (2010). [doi:10.1029/2009GL041436](https://doi.org/10.1029/2009GL041436)
66. S. M. Stanley, L. A. Hardie, Secular oscillations in the carbonate mineralogy of reef-building and sediment-producing organisms driven by tectonically forced shifts in seawater chemistry. *Palaeogeogr. Palaeoclimatol. Palaeoecol.* **144**, 3 (1998). [doi:10.1016/S0031-0182\(98\)00109-6](https://doi.org/10.1016/S0031-0182(98)00109-6)
67. J. B. Ries, Review: geological and experimental evidence for secular variation in seawater Mg/Ca (calcite-aragonite seas) and its effects on marine biological calcification. *Biogeosciences* **7**, 2795 (2010). [doi:10.5194/bg-7-2795-2010](https://doi.org/10.5194/bg-7-2795-2010)
68. C. Turley *et al.*, The societal challenge of ocean acidification. *Mar. Pollut. Bull.* **60**, 787 (2010). [doi:10.1016/j.marpolbul.2010.05.006](https://doi.org/10.1016/j.marpolbul.2010.05.006) [Medline](#)
69. N. Gruber, Warming up, turning sour, losing breath: ocean biogeochemistry under global change. *Philos. Trans. R. Soc. A-Math. Phys. Eng. Sci.* **369**, 1980 (2011). [doi:10.1098/rsta.2011.0003](https://doi.org/10.1098/rsta.2011.0003)
70. E. T. Sundquist, K. v. Visser, Elsevier, in *Treatise on Geochemistry: Biogeochemistry*, W. H. Schlesinger, Ed. (Elsevier, 2004), chap. 9.
71. J. A. D. Dickson, Fossil echinoderms as monitor of the Mg/Ca ratio of Phanerozoic oceans. *Science* **298**, 1222 (2002). [doi:10.1126/science.1075882](https://doi.org/10.1126/science.1075882) [Medline](#)
72. R. V. Demicco, T. K. Lowenstein, L. A. Hardie, R. J. Spencer, Model of seawater composition for the Phanerozoic. *Geology* **33**, 877 (2005). [doi:10.1130/G21945.1](https://doi.org/10.1130/G21945.1)

73. A. Ridgwell, A Mid Mesozoic Revolution in the regulation of ocean chemistry. *Mar. Geol.* **217**, 339 (2005). [doi:10.1016/j.margeo.2004.10.036](https://doi.org/10.1016/j.margeo.2004.10.036)
74. R. F. Weiss, Carbon dioxide in water and seawater: the solubility of a non-ideal gas. *Mar. Chem.* **2**, 203 (1974). [doi:10.1016/0304-4203\(74\)90015-2](https://doi.org/10.1016/0304-4203(74)90015-2)
75. F. J. Mojica Prieto, F. J. Millero, The values of $pK_1 + pK_2$ for the dissociation of carbonic acid in seawater. *Geochim. Cosmochim. Acta* **66**, 2529 (2002). [doi:10.1016/S0016-7037\(02\)00855-4](https://doi.org/10.1016/S0016-7037(02)00855-4)
76. D. A. Wolf-Gladrow, R. E. Zeebe, C. Klaas, A. Kötzinger, A. G. Dickson, Total alkalinity: The explicit conservative expression and its application to biogeochemical processes. *Mar. Chem.* **106**, 287 (2007). [doi:10.1016/j.marchem.2007.01.006](https://doi.org/10.1016/j.marchem.2007.01.006)
77. A. G. Dickson *et al.*, *PICES Special Publication* **3**, 191 (2007).
78. R. E. Zeebe, D. A. Wolf-Gladrow, *CO₂ in Seawater: Equilibrium, Kinetics, Isotopes*. Elsevier Oceanography Series (Elsevier, New York, 2001), vol. 65, pp. 1–346.
79. N. R. Edwards, M. R. *Clim. Dyn.* **24**, 415 (2005). [doi:10.1007/s00382-004-0508-8](https://doi.org/10.1007/s00382-004-0508-8)
80. A. Ridgwell *et al.*, Marine geochemical data assimilation in an efficient Earth System Model of global biogeochemical cycling. *Biogeosciences* **4**, 87 (2007). [doi:10.5194/bg-4-87-2007](https://doi.org/10.5194/bg-4-87-2007)
81. A. Ridgwell, J. Hargreaves, *Glob. Biogeochem. Cycle* **21**, GB2008 (2007).
82. D. Archer *et al.*, Atmospheric Lifetime of Fossil Fuel Carbon Dioxide. *Annu. Rev. Earth Planet. Sci.* **37**, 117 (2009). [doi:10.1146/annurev.earth.031208.100206](https://doi.org/10.1146/annurev.earth.031208.100206)
83. A. J. Ridgwell, thesis, Univ. of East Anglia at Norwich, UK (2001).
84. A. Ridgwell, Interpreting transient carbonate compensation depth changes by marine sediment core modeling. *Paleoceanography* **22**, PA4102 (2007). [doi:10.1029/2006PA001372](https://doi.org/10.1029/2006PA001372)
85. G. Munhoven, Glacial–interglacial changes of continental weathering: estimates of the related CO₂ and HCO₃⁻ flux variations and their uncertainties. *Global Planet. Change* **33**, 155 (2002). [doi:10.1016/S0921-8181\(02\)00068-1](https://doi.org/10.1016/S0921-8181(02)00068-1)
86. G. Colbourn, thesis, University of East Anglia, UK (2011).
87. R. A. Berner, GEOCARB II; a revised model of atmospheric CO₂ over Phanerozoic time. *Am. J. Sci.* **294**, 56 (1994). [doi:10.2475/ajs.294.1.56](https://doi.org/10.2475/ajs.294.1.56)
88. P. V. Brady, *J. Geophys. Res. Oceans* **96**, 18 (1991).
89. R. M. Key *et al.*, A global ocean carbon climatology: Results from Global Data Analysis Project (GLODAP). *Global Biogeochem. Cycles* **18**, GB4031 (2004). [doi:10.1029/2004GB002247](https://doi.org/10.1029/2004GB002247)
90. R. G. Najjar *et al.*, *Glob. Biogeochem. Cycle* **21**, GB3007 (2007).
91. R. A. Feely *et al.*, Impact of anthropogenic CO₂ on the CaCO₃ system in the oceans. *Science* **305**, 362 (2004). [doi:10.1126/science.1097329](https://doi.org/10.1126/science.1097329) Medline

92. A. Ridgwell, I. Zondervan, J. C. Hargreaves, J. Bijma, T. M. Lenton, Assessing the potential long-term increase of oceanic fossil fuel CO₂ uptake due to CO₂-calcification feedback. *Biogeosciences* **4**, 481 (2007). [doi:10.5194/bg-4-481-2007](https://doi.org/10.5194/bg-4-481-2007)
93. A. B. Colosimo *et al.*, in *Proc. ODP, Sci. Results*, T. J. Bralower, I. Premoli Silva, M. J. Malone, Eds. (2006), vol. 198, pp. 1–36.
94. S. Bains, R. M. Corfield, R. D. Norris, Mechanisms of climate warming at the end of the paleocene. *Science* **285**, 724 (1999). [doi:10.1126/science.285.5428.724](https://doi.org/10.1126/science.285.5428.724) [Medline](#)
95. E. Thomas *et al.*, in *Climate and Biota of the early Paleogene* (Salzburg, Austria, 2011).
96. E. Thomas, in *Causes and Consequences of Globally Warm Climates of the Paleogene*, S. Wing, P. Gingerich, B. Schmitz, E. Thomas, Eds. (Geologic Society of America, 2003), pp. 319–332.
97. J. C. Zachos *et al.*, A transient rise in tropical sea surface temperature during the Paleocene-Eocene thermal maximum. *Science* **302**, 1551 (2003). [doi:10.1126/science.1090110](https://doi.org/10.1126/science.1090110) [Medline](#)
98. C. M. John *et al.*, North American continental margin records of the Paleocene-Eocene thermal maximum: Implications for global carbon and hydrological cycling. *Paleoceanography* **23**, PA2217 (2008). [doi:10.1029/2007PA001465](https://doi.org/10.1029/2007PA001465)
99. P. Stassen *et al.*, *J. Micropalaentol.*, 10.1144/0262-821X11-026 (2012).
100. A. Sluijs *et al.*, Environmental precursors to rapid light carbon injection at the Palaeocene/Eocene boundary. *Nature* **450**, 1218 (2007). [doi:10.1038/nature06400](https://doi.org/10.1038/nature06400) [Medline](#)
101. G. R. Dickens, J. R. O’Neil, D. K. Rea, R. M. Owen, Dissociation of oceanic methane hydrate as a cause of the carbon isotope excursion at the end of the Paleocene. *Paleoceanography* **10**, 965 (1995). [doi:10.1029/95PA02087](https://doi.org/10.1029/95PA02087)
102. P. B. Wignall, Large igneous provinces and mass extinctions. *Earth Sci. Rev.* **53**, 1 (2001). [doi:10.1016/S0012-8252\(00\)00037-4](https://doi.org/10.1016/S0012-8252(00)00037-4)
103. G. De’ath, J. M. Lough, K. E. Fabricius, Declining coral calcification on the Great Barrier Reef. *Science* **323**, 116 (2009). [doi:10.1126/science.1165283](https://doi.org/10.1126/science.1165283) [Medline](#)
104. H. de Moel *et al.*, Planktic foraminiferal shell thinning in the Arabian Sea due to anthropogenic ocean acidification? *Biogeosciences* **6**, 1917 (2009). [doi:10.5194/bg-6-1917-2009](https://doi.org/10.5194/bg-6-1917-2009)
105. A. Indermühle *et al.*, *Nature* **398**, 121 (1999). [doi:10.1038/18158](https://doi.org/10.1038/18158)
106. P. Tans, R. Keeling, www.esrl.noaa.gov/gmd/ccgg/trends. (2010).
107. N. R. Bates, Interannual variability of the oceanic CO₂ sink in the subtropical gyre of the North Atlantic Ocean over the last 2 decades. *J. Geophys. Res. Oceans* **112**, (C9), C09013 (2007). [doi:10.1029/2006JC003759](https://doi.org/10.1029/2006JC003759)
108. J. A. Kleypas *et al.*, “Impacts of Ocean Acidification on Coral Reefs and Other Marine Calcifiers: A Guide for Future Research, report of a workshop held 18–20 April 2005, St. Petersburg, FL” (NSF, NOAA, and the U.S. Geological Survey, Washington, DC, 2006).

109. D. K. Gledhill, R. Wanninkhof, F. J. Millero, M. Eakin, Ocean acidification of the Greater Caribbean Region 1996–2006. *J. Geophys. Res. Oceans* **113**, (C10), C10031 (2008). [doi:10.1029/2007JC004629](https://doi.org/10.1029/2007JC004629)
110. N. A. Rayner *et al.*, Improved analyses of changes and uncertainties in sea surface temperature measured in situ since the mid-nineteenth century: The HadSST2 dataset. *J. Clim.* **19**, 446 (2006). [doi:10.1175/JCLI3637.1](https://doi.org/10.1175/JCLI3637.1)
111. G. L. Foster, Seawater pH, pCO₂ and [CO₂–3] variations in the Caribbean Sea over the last 130 kyr: A boron isotope and B/Ca study of planktic foraminifera. *Earth Planet. Sci. Lett.* **271**, 254 (2008). [doi:10.1016/j.epsl.2008.04.015](https://doi.org/10.1016/j.epsl.2008.04.015)
112. MARGO Project members, *Nat. Geosci.* **2**, 127 (2009). [doi:10.1038/ngeo411](https://doi.org/10.1038/ngeo411)
113. H. Pälike *et al.*, The heartbeat of the Oligocene climate system. *Science* **314**, 1894 (2006). [doi:10.1126/science.1133822](https://doi.org/10.1126/science.1133822) [Medline](#)
114. A. Holbourn, W. Kuhnt, M. Schulz, J.-A. Flores, N. Andersen, Orbitally-paced climate evolution during the middle Miocene “Monterey” carbon-isotope excursion. *Earth Planet. Sci. Lett.* **261**, 534 (2007). [doi:10.1016/j.epsl.2007.07.026](https://doi.org/10.1016/j.epsl.2007.07.026)
115. M. Pagani, J. C. Zachos, K. H. Freeman, B. Tipple, S. Bohaty, Marked decline in atmospheric carbon dioxide concentrations during the Paleogene. *Science* **309**, 600 (2005). [doi:10.1126/science.1110063](https://doi.org/10.1126/science.1110063) [Medline](#)
116. H. J. Dowsett *et al.*, Middle Pliocene sea surface temperature variability. *Paleoceanography* **20**, PA2014 (2005). [doi:10.1029/2005PA001133](https://doi.org/10.1029/2005PA001133)
117. K. T. Lawrence, T. D. Herbert, C. M. Brown, M. E. Raymo, A. M. Haywood, High-amplitude variations in North Atlantic sea surface temperature during the early Pliocene warm period. *Paleoceanography* **24**, PA2218 (2009). [doi:10.1029/2008PA001669](https://doi.org/10.1029/2008PA001669)
118. B. P. Flower, J. P. Kennett, Middle Miocene ocean-climate transition: High-resolution oxygen and carbon isotopic records from Deep Sea Drilling Project Site 588A, southwest Pacific. *Paleoceanography* **8**, 811 (1993). [doi:10.1029/93PA02196](https://doi.org/10.1029/93PA02196)
119. B. P. Flower, J. P. Kennett, The middle Miocene climatic transition: East Antarctic ice sheet development, deep ocean circulation and global carbon cycling. *Palaeogeogr. Palaeoclimatol. Palaeoecol.* **108**, 537 (1994). [doi:10.1016/0031-0182\(94\)90251-8](https://doi.org/10.1016/0031-0182(94)90251-8)
120. B. P. Flower, J. P. Kennett, Middle Miocene deepwater paleoceanography in the southwest Pacific: Relations with East Antarctic Ice Sheet development. *Paleoceanography* **10**, 1095 (1995). [doi:10.1029/95PA02022](https://doi.org/10.1029/95PA02022)
121. L. Stap, A. Sluijs, E. Thomas, L. Lourens, Patterns and magnitude of deep sea carbonate dissolution during Eocene Thermal Maximum 2 and H2, Walvis Ridge, southeastern Atlantic Ocean. *Paleoceanography* **24**, PA1211 (2009). [doi:10.1029/2008PA001655](https://doi.org/10.1029/2008PA001655)
122. H. Svensen *et al.*, Release of methane from a volcanic basin as a mechanism for initial Eocene global warming. *Nature* **429**, 542 (2004). [doi:10.1038/nature02566](https://doi.org/10.1038/nature02566) [Medline](#)
123. D. C. Kelly, T. J. Bralower, J. C. Zachos, Evolutionary consequences of the latest Paleocene thermal maximum for tropical planktonic foraminifera. *Palaeogeogr. Palaeoclimatol. Palaeoecol.* **141**, 139 (1998). [doi:10.1016/S0031-0182\(98\)00017-0](https://doi.org/10.1016/S0031-0182(98)00017-0)

124. J. Uchikawa, R. E. Zeebe, Examining possible effects of seawater pH decline on foraminiferal stable isotopes during the Paleocene-Eocene Thermal Maximum. *Paleoceanography* **25**, PA2216 (2010). [doi:10.1029/2009PA001864](https://doi.org/10.1029/2009PA001864)
125. A. A. Ekdale, R. G. Bromley, *J. Sediment. Petrol.* **54**, 681 (1984).
126. W. Kiessling, P. A. Claeys, in *Geological and biological effects of impact events*, E. Buffetaut, C. Koeberl, Eds. (Springer, Berlin, 2001), pp. 33–140.
127. D. J. Beerling, B. H. Lomax, D. L. Royer, G. R. Upchurch, Jr., L. R. Kump, An atmospheric pCO₂ reconstruction across the Cretaceous-Tertiary boundary from leaf megafossils. *Proc. Natl. Acad. Sci. U.S.A.* **99**, 7836 (2002). [doi:10.1073/pnas.122573099](https://doi.org/10.1073/pnas.122573099) [Medline](#)
128. S. D'Hondt, consequences of the Cretaceous/Paleogene mass extinction for marine ecosystems. *Annu. Rev. Ecol. Evol. Syst.* **36**, 295 (2005). [doi:10.1146/annurev.ecolsys.35.021103.105715](https://doi.org/10.1146/annurev.ecolsys.35.021103.105715)
129. H. Brinkhuis, J. P. Bujak, J. Smit, G. J. M. Versteegh, H. Visscher, Dinoflagellate-based sea surface temperature reconstructions across the Cretaceous–Tertiary boundary. *Palaeogeogr. Palaeoclimatol. Palaeoecol.* **141**, 67 (1998). [doi:10.1016/S0031-0182\(98\)00004-2](https://doi.org/10.1016/S0031-0182(98)00004-2)
130. K. L. Bice *et al.*, A multiple proxy and model study of Cretaceous upper ocean temperatures and atmospheric CO₂ concentrations. *Paleoceanography* **21**, PA2002 (2006). [doi:10.1029/2005PA001203](https://doi.org/10.1029/2005PA001203)
131. A. Forster, S. Schouten, K. Moriya, P. A. Wilson, J. S. Sinninghe Damsté, Tropical warming and intermittent cooling during the Cenomanian/Turonian oceanic anoxic event 2: Sea surface temperature records from the equatorial Atlantic. *Paleoceanography* **22**, PA1219 (2007). [doi:10.1029/2006PA001349](https://doi.org/10.1029/2006PA001349)
132. J. Erbacher, B. T. Huber, R. D. Norris, M. Markey, Increased thermohaline stratification as a possible cause for an ocean anoxic event in the Cretaceous period. *Nature* **409**, 325 (2001). [doi:10.1038/35053041](https://doi.org/10.1038/35053041) [Medline](#)
133. M. F. Schaller, J. D. Wright, D. V. Kent, Atmospheric PCO₂ perturbations associated with the Central Atlantic Magmatic Province. *Science* **331**, 1404 (2011). [doi:10.1126/science.1199011](https://doi.org/10.1126/science.1199011) [Medline](#)
134. W. Kiessling *et al.*, *Facies* **24**, 657 (2009).
135. J. C. McElwain, D. J. Beerling, F. I. Woodward, Fossil plants and global warming at the Triassic–Jurassic boundary. *Science* **285**, 1386 (1999). [doi:10.1126/science.285.5432.1386](https://doi.org/10.1126/science.285.5432.1386) [Medline](#)
136. C. Korte, S. P. Hesselbo, H. C. Jenkyns, R. E. M. Rickaby, C. Spotl, Palaeoenvironmental significance of carbon- and oxygen-isotope stratigraphy of marine Triassic–Jurassic boundary sections in SW Britain. *J. Geol. Soc. London* **166**, 431 (2009). [doi:10.1144/0016-76492007-177](https://doi.org/10.1144/0016-76492007-177)
137. S. L. Kamo *et al.*, Rapid eruption of Siberian flood-volcanic rocks and evidence for coincidence with the Permian–Triassic boundary and mass extinction at 251 Ma. *Earth Planet. Sci. Lett.* **214**, 75 (2003). [doi:10.1016/S0012-821X\(03\)00347-9](https://doi.org/10.1016/S0012-821X(03)00347-9)

138. J. L. Payne *et al.*, Erosional truncation of uppermost Permian shallow-marine carbonates and implications for Permian-Triassic boundary events. *Geol. Soc. Am. Bull.* **119**, 771 (2007). [doi:10.1130/B26091.1](https://doi.org/10.1130/B26091.1)
139. M. E. Clapham, J. L. Payne, Acidification, anoxia, and extinction: A multiple logistic regression analysis of extinction selectivity during the Middle and Late Permian. *Geology* **39**, 1059 (2011). [doi:10.1130/G32230.1](https://doi.org/10.1130/G32230.1)
140. H. Svensen *et al.*, Siberian gas venting and the end-Permian environmental crisis. *Earth Planet. Sci. Lett.* **277**, 490 (2009). [doi:10.1016/j.epsl.2008.11.015](https://doi.org/10.1016/j.epsl.2008.11.015)
141. D. L. Kidder, T. R. Worsley, Causes and consequences of extreme Permo-Triassic warming to globally equitable climate and relation to the Permo-Triassic extinction and recovery. *Palaeogeogr. Palaeoclimatol. Palaeoecol.* **203**, 207 (2004). [doi:10.1016/S0031-0182\(03\)00667-9](https://doi.org/10.1016/S0031-0182(03)00667-9)
142. D. D. Ekart *et al.*, A 400 million year carbon isotope record of pedogenic carbonate; implications for paleoatmospheric carbon dioxide. *Am. J. Sci.* **299**, 805 (1999). [doi:10.2475/ajs.299.10.805](https://doi.org/10.2475/ajs.299.10.805)
143. N. J. Tabor, C. J. Yapp, I. P. Montañez, Goethite, calcite, and organic matter from Permian and Triassic soils: carbon isotopes and CO₂ concentrations 1. *Geochim. Cosmochim. Acta* **68**, 1503 (2004). [doi:10.1016/S0016-7037\(03\)00497-6](https://doi.org/10.1016/S0016-7037(03)00497-6)
144. I. P. Montañez *et al.*, CO₂-forced climate and vegetation instability during Late Paleozoic deglaciation. *Science* **315**, 87 (2007). [doi:10.1126/science.1134207](https://doi.org/10.1126/science.1134207) [Medline](#)
145. D. O. Breecker, Z. D. Sharp, L. D. McFadden, Seasonal bias in the formation and stable isotopic composition of pedogenic carbonate in modern soils from central New Mexico, USA. *Geol. Soc. Am. Bull.* **121**, 630 (2009). [doi:10.1130/B26413.1](https://doi.org/10.1130/B26413.1)
146. J. R. Rustad, E. J. Bylaska, V. E. Jackson, D. A. Dixon, Calculation of boron-isotope fractionation between B(OH)₃(aq) and B(OH)₄-(aq). *Geochim. Cosmochim. Acta* **74**, 2843 (2010). [doi:10.1016/j.gca.2010.02.032](https://doi.org/10.1016/j.gca.2010.02.032)
147. P. N. Pearson, M. R. Palmer, Atmospheric carbon dioxide concentrations over the past 60 million years. *Nature* **406**, 695 (2000). [doi:10.1038/35021000](https://doi.org/10.1038/35021000) [Medline](#)
148. D. L. Royer, R. A. Berner, D. J. Beerling, Phanerozoic atmospheric CO₂ change: evaluating geochemical and paleobiological approaches. *Earth Sci. Rev.* **54**, 349 (2001). [doi:10.1016/S0012-8252\(00\)00042-8](https://doi.org/10.1016/S0012-8252(00)00042-8)
149. M. Pagani, D. Lemarchand, A. Spivack, J. Gaillardet, A critical evaluation of the boron isotope-pH proxy: The accuracy of ancient ocean pH estimates. *Geochim. Cosmochim. Acta* **69**, 953 (2005). [doi:10.1016/j.gca.2004.07.029](https://doi.org/10.1016/j.gca.2004.07.029)
150. P. N. Pearson *et al.*, Warm tropical sea surface temperatures in the Late Cretaceous and Eocene epochs. *Nature* **413**, 481 (2001). [doi:10.1038/35097000](https://doi.org/10.1038/35097000) [Medline](#)
151. A. K. Tripati, C. D. Roberts, R. A. Eagle, Coupling of CO₂ and ice sheet stability over major climate transitions of the last 20 million years. *Science* **326**, 1394 (2009). [doi:10.1126/science.1178296](https://doi.org/10.1126/science.1178296) [Medline](#)

152. J. Yu, H. Elderfield, B. Höönsch, B/Ca in planktonic foraminifera as a proxy for surface seawater pH. *Paleoceanography* **22**, PA2202 (2007). [doi:10.1029/2006PA001347](https://doi.org/10.1029/2006PA001347)
153. K. A. Allen *et al.*, Controls on boron incorporation in cultured tests of the planktic foraminifer *Orbulina universa*. *Earth Planet. Sci. Lett.* **309**, 291 (2011). [doi:10.1016/j.epsl.2011.07.010](https://doi.org/10.1016/j.epsl.2011.07.010)
154. D. J. Beerling, D. L. Royer, Fossil plants as indicators of the Phanerozoic global carbon cycle. *Annu. Rev. Earth Planet. Sci.* **30**, 527 (2002). [doi:10.1146/annurev.earth.30.091201.141413](https://doi.org/10.1146/annurev.earth.30.091201.141413)
155. B. J. Tipple, S. R. Meyers, M. Pagani, Carbon isotope ratio of Cenozoic CO₂: A comparative evaluation of available geochemical proxies. *Paleoceanography* **25**, PA3202 (2010). [doi:10.1029/2009PA001851](https://doi.org/10.1029/2009PA001851)
156. *A Geologic Time Scale*. F. M. Gradstein, J. G. Ogg, A. G. Smith, Eds., (Cambridge Univ Press, Cambridge, 2004).
157. R. K. Schecki *et al.*, *J. Sediment. Petrol.* **58**, 801 (1988).
158. K. H. Freeman, J. M. Hayes, Fractionation of carbon isotopes by phytoplankton and estimates of ancient CO₂ levels. *Global Biogeochem. Cycles* **6**, 185 (1992). [doi:10.1029/92GB00190](https://doi.org/10.1029/92GB00190) [Medline](#)
159. J. Van Der Burgh, H. Visscher, D. L. Dilcher, W. M. Kürschner, Paleoatmospheric signatures in neogene fossil leaves. *Science* **260**, 1788 (1993). [doi:10.1126/science.260.5115.1788](https://doi.org/10.1126/science.260.5115.1788) [Medline](#)
160. W. M. Kürschner, J. van der Burgh, H. Visscher, D. L. Dilcher, Oak leaves as biosensors of late neogene and early pleistocene paleoatmospheric CO₂ concentrations. *Mar. Micropaleontol.* **27**, 299 (1996). [doi:10.1016/0377-8398\(95\)00067-4](https://doi.org/10.1016/0377-8398(95)00067-4)
161. B. Höönsch, N. G. Hemming, D. Archer, M. Siddall, J. F. McManus, Atmospheric carbon dioxide concentration across the mid-Pleistocene transition. *Science* **324**, 1551 (2009). [doi:10.1126/science.1171477](https://doi.org/10.1126/science.1171477) [Medline](#)
162. B. J. Fletcher, S. J. Brentnall, C. W. Anderson, R. A. Berner, D. J. Beerling, Atmospheric carbon dioxide linked with Mesozoic and early Cenozoic climate change. *Nat. Geosci.* **1**, 43 (2008). [doi:10.1038/ngeo.2007.29](https://doi.org/10.1038/ngeo.2007.29)
163. T. K. Lowenstein, R. V. Demicco, Elevated Eocene atmospheric CO₂ and its subsequent decline. *Science* **313**, 1928 (2006). [doi:10.1126/science.1129555](https://doi.org/10.1126/science.1129555) [Medline](#)
164. N. H. Platt, Lacustrine carbonates and pedogenesis: sedimentology and origin of palustrine deposits from the Early Cretaceous Rupel Formation, W Cameros Basin, N Spain. *Sedimentology* **36**, 665 (1989). [doi:10.1111/j.1365-3091.1989.tb02092.x](https://doi.org/10.1111/j.1365-3091.1989.tb02092.x)
165. L. D. Stott, Higher temperatures and lower oceanic pCO₂: A climate enigma at the end of the Paleocene Epoch. *Paleoceanography* **7**, 395 (1992). [doi:10.1029/92PA01183](https://doi.org/10.1029/92PA01183)
166. D. J. Beerling *et al.*, Short communication. Stomatal responses of the ‘living fossil’ *Ginkgo biloba* L. to changes in atmospheric CO₂ concentrations. *J. Exp. Bot.* **49**, 1603 (1998). [doi:10.1093/jexbot/49.326.1603](https://doi.org/10.1093/jexbot/49.326.1603)

167. T. E. Cerling, Carbon dioxide in the atmosphere; Evidence from Cenozoic and Mesozoic Paleosols. *Am. J. Sci.* **291**, 377 (1991). [doi:10.2475/ajs.291.4.377](https://doi.org/10.2475/ajs.291.4.377)
168. M. Pagani, M. A. Arthur, K. H. Freeman, Miocene evolution of atmospheric carbon dioxide. *Paleoceanography* **14**, 273 (1999). [doi:10.1029/1999PA900006](https://doi.org/10.1029/1999PA900006)
169. M. Pagani, K. H. Freeman, M. A. Arthur, Late miocene atmospheric CO₂ concentrations and the expansion of C(4) grasses. *Science* **285**, 876 (1999).
[doi:10.1126/science.285.5429.876](https://doi.org/10.1126/science.285.5429.876) [Medline](#)
170. J. Henderiks, M. Pagani, Coccolithophore cell size and the Paleogene decline in atmospheric CO₂. *Earth Planet. Sci. Lett.* **269**, 576 (2008).
[doi:10.1016/j.epsl.2008.03.016](https://doi.org/10.1016/j.epsl.2008.03.016)
171. J. C. McElwain, Do fossil plants signal palaeoatmospheric carbon dioxide concentration in the geological past? *Philos. Trans. R. Soc. Lond. B Biol. Sci.* **353**, 83 (1998).
[doi:10.1098/rstb.1998.0193](https://doi.org/10.1098/rstb.1998.0193)
172. P. N. Pearson, G. L. Foster, B. S. Wade, Atmospheric carbon dioxide through the Eocene-Oligocene climate transition. *Nature* **461**, 1110 (2009). [doi:10.1038/nature08447](https://doi.org/10.1038/nature08447) [Medline](#)
173. P. L. Koch, J. C. Zachos, P. D. Gingerich, Correlation between isotope records in marine and continental carbon reservoirs near the Palaeocene/Eocene boundary. *Nature* **358**, 319 (1992). [doi:10.1038/358319a0](https://doi.org/10.1038/358319a0)
174. P. Muchez, C. Peeters, E. Keppens, W. A. Viaene, Stable isotopic composition of paleosols in the Lower Viséan of eastern Belgium: Evidence of evaporation and soil-gas CO₂. *Chem. Geol.* **106**, 389 (1993). [doi:10.1016/0009-2541\(93\)90039-L](https://doi.org/10.1016/0009-2541(93)90039-L)
175. L.-Q. Chen *et al.*, Assessing the potential for the stomatal characters of extant and fossil Ginkgo leaves to signal atmospheric CO₂ change. *Am. J. Bot.* **88**, 1309 (2001).
[doi:10.2307/3558342](https://doi.org/10.2307/3558342) [Medline](#)
176. A. Sinha, L. D. Stott, New atmospheric pCO₂ estimates from palesols during the late Paleocene/early Eocene global warming interval. *Global Planet. Change* **9**, 297 (1994).
[doi:10.1016/0921-8181\(94\)00010-7](https://doi.org/10.1016/0921-8181(94)00010-7)
177. W. M. Kürschner *et al.*, in *Geological Perspectives of Global Climate Change*, L. C. Gerhard, W. E. Harrison, B. M. Hanson, Eds. (The American Association of Petroleum Geologists, Tulsa, 2001), vol. 47, pp. 169–189.
178. J. E. Andrews, S. K. Tandon, P. F. Dennis, Concentration of carbon dioxide in the Late Cretaceous atmosphere. *J. Geol. Soc. London* **152**, 1 (1995).
[doi:10.1144/gsjgs.152.1.0001](https://doi.org/10.1144/gsjgs.152.1.0001)
179. D. L. Royer *et al.*, Paleobotanical evidence for near present-day levels of atmospheric Co₂ during part of the tertiary. *Science* **292**, 2310 (2001). [doi:10.1126/science.292.5525.2310](https://doi.org/10.1126/science.292.5525.2310) [Medline](#)
180. D. J. Beerling, A. Fox, C. W. Anderson, Quantitative uncertainty analyses of ancient atmospheric CO₂ estimates from fossil leaves. *Am. J. Sci.* **309**, 775 (2009).
[doi:10.2475/09.2009.01](https://doi.org/10.2475/09.2009.01)

181. C. I. Mora, S. G. Driese, L. A. Colarusso, Middle to Late Paleozoic Atmospheric CO₂ Levels from Soil Carbonate and Organic Matter. *Science* **271**, 1105 (1996). [doi:10.1126/science.271.5252.1105](https://doi.org/10.1126/science.271.5252.1105)
182. D. J. Beerling, Low atmospheric CO(2) levels during the Permo- Carboniferous glaciation inferred from fossil lycopsids. *Proc. Natl. Acad. Sci. U.S.A.* **99**, 12567 (2002). [doi:10.1073/pnas.202304999](https://doi.org/10.1073/pnas.202304999) [Medline](#)
183. Y. I. Lee, Stable isotopic composition of calcic paleosols of the Early Cretaceous Hasandong Formation, southeastern Korea. *Palaeogeogr. Palaeoclimatol. Palaeoecol.* **150**, 123 (1999). [doi:10.1016/S0031-0182\(99\)00010-3](https://doi.org/10.1016/S0031-0182(99)00010-3)
184. Y. I. Lee, K. Hisada, Stable isotopic composition of pedogenic carbonates of the Early Cretaceous Shimonoseki Subgroup, western Honshu, Japan. *Palaeogeogr. Palaeoclimatol. Palaeoecol.* **153**, 127 (1999). [doi:10.1016/S0031-0182\(99\)00069-3](https://doi.org/10.1016/S0031-0182(99)00069-3)
185. D. L. Royer, in *Causes and Consequences of Globally Warm Climates in the Early Paleogene*, S. L. Wing, P. D. Gingerich, B. Schmitz, E. Thomas, Eds. (Geological Society of America Special Paper 369, Boulder, 2003), vol. 369, pp. 79–93.
186. S. G. Driese *et al.*, in *Phanerozoic Terrestrial Ecosystems*, R. A. Gastaldo, W. A. DiMichele, Eds. (Paleontological Society Special Papers 6, 2000), pp. 47–61.
187. D. R. Greenwood, M. J. Scarr, D. C. Christophe, Leaf stomatal frequency in the Australian tropical rainforest tree Neolitsea dealbata (Lauraceae) as a proxy measure of atmospheric pCO₂. *Palaeogeogr. Palaeoclimatol. Palaeoecol.* **196**, 375 (2003). [doi:10.1016/S0031-0182\(03\)00465-6](https://doi.org/10.1016/S0031-0182(03)00465-6)
188. J. E. Cox *et al.*, *Northeast. Geol. Environ. Sci.* **23**, 91 (2001).
189. A. Roth-Nebelsick, W. Konrad, Assimilation and transpiration capabilities of rhyniophytic plants from the Lower Devonian and their implications for paleoatmospheric CO₂ concentration. *Palaeogeogr. Palaeoclimatol. Palaeoecol.* **202**, 153 (2003). [doi:10.1016/S0031-0182\(03\)00634-5](https://doi.org/10.1016/S0031-0182(03)00634-5)
190. J. C. McElwain, J. Wade-Murphy, S. P. Hesselbo, Changes in carbon dioxide during an oceanic anoxic event linked to intrusion into Gondwana coals. *Nature* **435**, 479 (2005). [doi:10.1038/nature03618](https://doi.org/10.1038/nature03618) [Medline](#)
191. L. H. Tanner, J. F. Hubert, B. P. Coffey, D. P. McInerney, Stability of atmospheric CO₂ levels across the Triassic/Jurassic boundary. *Nature* **411**, 675 (2001). [doi:10.1038/35079548](https://doi.org/10.1038/35079548) [Medline](#)
192. M. Haworth, S. P. Hesselbo, J. C. McElwain, S. A. Robinson, J. W. Brunt, Mid-Cretaceous pCO₂ based on stomata of the extinct conifer Pseudofrenelopsis (Cheirolepidiaceae). *Geology* **33**, 749 (2005). [doi:10.1130/G21736.1](https://doi.org/10.1130/G21736.1)
193. S. A. Robinson *et al.*, Atmospheric pCO₂ and depositional environment from stable-isotope geochemistry of calcrete nodules (Barremian, Lower Cretaceous, Wealden Beds, England). *J. Geol. Soc. London* **159**, 215 (2002). [doi:10.1144/0016-764901-015](https://doi.org/10.1144/0016-764901-015)
194. B. Sun *et al.*, *Acta Geol. Sin.* **81**, 931 (2007). [doi:10.1111/j.1755-6724.2007.tb01016.x](https://doi.org/10.1111/j.1755-6724.2007.tb01016.x)

195. L. Nordt, S. Atchley, S. I. Dworkin, Paleosol barometer indicates extreme fluctuations in atmospheric CO₂ across the Cretaceous-Tertiary boundary. *Geology* **30**, 703 (2002). [doi:10.1130/0091-7613\(2002\)030<0703:PBIEFI>2.0.CO;2](https://doi.org/10.1130/0091-7613(2002)030<0703:PBIEFI>2.0.CO;2)
196. W. M. Kürschner, Z. Kvacek, D. L. Dilcher, The impact of Miocene atmospheric carbon dioxide fluctuations on climate and the evolution of terrestrial ecosystems. *Proc. Natl. Acad. Sci. U.S.A.* **105**, 449 (2008). [doi:10.1073/pnas.0708588105](https://doi.org/10.1073/pnas.0708588105) [Medline](#)
197. L. Nordt, S. Atchley, S. Dworkin, Terrestrial evidence for two greenhouse events in the latest Cretaceous. *GSA Today* **13**, 4 (2003). [doi:10.1130/1052-5173\(2003\)013<4:TEFTGE>2.0.CO;2](https://doi.org/10.1130/1052-5173(2003)013<4:TEFTGE>2.0.CO;2)
198. C. Quan, C. Sun, Y. Sun, G. Sun, High resolution estimates of paleo-CO₂ levels through the Campanian (Late Cretaceous) based on Ginkgo cuticles. *Cretac. Res.* **30**, 424 (2009). [doi:10.1016/j.cretres.2008.08.004](https://doi.org/10.1016/j.cretres.2008.08.004)
199. P. Ghosh *et al.*, in *A History of Atmospheric CO₂ and Its Effects on Plants, Animals, and Ecosystems*, J. R. Ehleringer, T. E. Cerling, M. D. Dearing, Eds. (Springer, New York, 2005), pp. 8–34.
200. M. G. Passalia, Cretaceous pCO₂ estimation from stomatal frequency analysis of gymnosperm leaves of Patagonia, Argentina. *Palaeogeogr. Palaeoclimatol. Palaeoecol.* **273**, 17 (2009). [doi:10.1016/j.palaeo.2008.11.010](https://doi.org/10.1016/j.palaeo.2008.11.010)
201. S. J. Prochnow, L. C. Nordt, S. C. Atchley, M. R. Hudec, Multi-proxy paleosol evidence for middle and late Triassic climate trends in eastern Utah. *Palaeogeogr. Palaeoclimatol. Palaeoecol.* **232**, 53 (2006). [doi:10.1016/j.palaeo.2005.08.011](https://doi.org/10.1016/j.palaeo.2005.08.011)
202. G. J. Retallack, Greenhouse crises of the past 300 million years. *Geol. Soc. Am. Bull.* **121**, 1441 (2009). [doi:10.1130/B26341.1](https://doi.org/10.1130/B26341.1)
203. A. Sandler, in *Paleoenvironmental Record and Applications of Calcretes and Palustrine Carbonates*, A. M. Alonso-Zarza, L. H. Tanner, Eds. (Geological Society of America Special Paper, Boulder, 2006), vol. 416, pp. 75–88.
204. D. F. Yan *et al.*, Science in China Series D. *Earth Sci.* **52**, 2029 (2009).
205. I. P. Montañez *et al.*, CO₂-forced climate and vegetation instability during Late Paleozoic deglaciation. *Science* **315**, 87 (2007). [doi:10.1126/science.1134207](https://doi.org/10.1126/science.1134207) [Medline](#)
206. R. S. Barclay, J. C. McElwain, B. B. Sageman, Carbon sequestration activated by a volcanic CO₂ pulse during Ocean Anoxic Event 2. *Nat. Geosci.* **3**, 205 (2010). [doi:10.1038/ngeo757](https://doi.org/10.1038/ngeo757)
207. D. M. Cleveland, L. C. Nordt, S. I. Dworkin, S. C. Atchley, Pedogenic carbonate isotopes as evidence for extreme climatic events preceding the Triassic-Jurassic boundary: Implications for the biotic crisis? *Geol. Soc. Am. Bull.* **120**, 1408 (2008). [doi:10.1130/B26332.1](https://doi.org/10.1130/B26332.1)
208. R. Y. Smith, D. R. Greenwood, J. F. Basinger, Estimating paleoatmospheric pCO₂ during the Early Eocene Climatic Optimum from stomatal frequency of Ginkgo, Okanagan Highlands, British Columbia, Canada. *Palaeogeogr. Palaeoclimatol. Palaeoecol.* **293**, 120 (2010). [doi:10.1016/j.palaeo.2010.05.006](https://doi.org/10.1016/j.palaeo.2010.05.006)

209. G. J. Retallack, Refining a pedogenic-carbonate CO₂ paleobarometer to quantify a middle Miocene greenhouse spike. *Palaeogeogr. Palaeoclimatol. Palaeoecol.* **281**, 57 (2009). [doi:10.1016/j.palaeo.2009.07.011](https://doi.org/10.1016/j.palaeo.2009.07.011)
210. N. R. Bonis, J. H. A. Van Konijnenburg-Van Cittert, W. M. Kürschner, Changing CO₂ conditions during the end-Triassic inferred from stomatal frequency analysis on *Lepidopteris ottonis* (Goeppert) Schimper and *Ginkgoites taeniatus* (Braun) Harris. *Palaeogeogr. Palaeoclimatol. Palaeoecol.* **295**, 146 (2010). [doi:10.1016/j.palaeo.2010.05.034](https://doi.org/10.1016/j.palaeo.2010.05.034)
211. A. Leier, J. Quade, P. DeCelles, P. Kapp, Stable isotopic results from paleosol carbonate in South Asia: Paleoenvironmental reconstructions and selective alteration. *Earth Planet. Sci. Lett.* **279**, 242 (2009). [doi:10.1016/j.epsl.2008.12.044](https://doi.org/10.1016/j.epsl.2008.12.044)
212. G. Doria *et al.*, Declining atmospheric CO₂ during the late Middle Eocene climate transition. *Am. J. Sci.* **311**, 63 (2011). [doi:10.2475/01.2011.03](https://doi.org/10.2475/01.2011.03)
213. R. A. MacRae, R. A. Fensome, G. L. Williams, Fossil dinoflagellate diversity, originations, and extinctions and their significance. *Can. J. Bot.* **74**, 1687 (1996). [doi:10.1139/b96-205](https://doi.org/10.1139/b96-205)
214. M. B. Hart *et al.*, The search for the origin of the planktic Foraminifera. *J. Geol. Soc. London* **160**, 341 (2003). [doi:10.1144/0016-764903-003](https://doi.org/10.1144/0016-764903-003)
215. R. E. Martin, Cyclic and secular variation in microfossil biomineralization: Clues to the biogeochemical evolution of Phanerozoic oceans. *Global Planet. Change* **11**, 1 (1995). [doi:10.1016/0921-8181\(94\)00011-2](https://doi.org/10.1016/0921-8181(94)00011-2)
216. T. H. G. Ezard, T. Aze, P. N. Pearson, A. Purvis, Interplay between changing climate and species' ecology drives macroevolutionary dynamics. *Science* **332**, 349 (2011). [doi:10.1126/science.1203060](https://doi.org/10.1126/science.1203060) [Medline](#)
217. M. E. Clapham, S. Shen, D. J. Bottjer, The double mass extinction revisited: reassessing the severity, selectivity, and causes of the end-Guadalupian biotic crisis (Late Permian). *Paleobiology* **35**, 32 (2009). [doi:10.1666/08033.1](https://doi.org/10.1666/08033.1)